

Drug-induced DNA repair: X-ray structure of a DNA–ditercalinium complex

QI GAO*, LOREN DEAN WILLIAMS*, MARTIN EGLI*, DOV RABINOVICH*†, SHUN-LE CHEN‡, GARY J. QUIGLEY‡, AND ALEXANDER RICH*

*Department of Biology, Massachusetts Institute of Technology, Cambridge, MA 02139; and †Department of Chemistry, Hunter College, New York, NY 10021

Contributed by Alexander Rich, December 26, 1990

ABSTRACT Ditercalinium is a synthetic anticancer drug that binds to DNA by bis-intercalation and activates DNA repair processes. In prokaryotes, noncovalent DNA–ditercalinium complexes are incorrectly recognized by the *uvrABC* repair system as covalent lesions on DNA. In eukaryotes, mitochondrial DNA is degraded by excess and futile DNA repair. Using x-ray crystallography, we have determined, to 1.7 Å resolution, the three-dimensional structure of a complex of ditercalinium bound to the double-stranded DNA fragment [d(CGCG)]₂. The DNA in the complex with ditercalinium is kinked (by 15°) and severely unwound (by 36°) with exceptionally wide major and minor grooves. Recognition of the DNA–ditercalinium complex by *uvrABC* in prokaryotes, and by mitochondrial DNA repair systems in eukaryotes, might be related to drug-induced distortion of the DNA helix.

DNA is a classical target for antibiotics and anticancer drugs. Drugs that bind to DNA and inhibit replication and transcription have found wide clinical use. Other aspects of DNA processing also constitute attractive targets for therapeutic agents. DNA repair systems are a relatively recent and almost unexplored area for therapeutic agents. Repair systems correct damage inflicted on DNA by incorrect synthesis, reactive chemical agents, ionizing radiation, and spontaneous reactions such as deamination of cytosine (1). Recently, agents have been discovered that bind noncovalently to DNA but still activate DNA repair systems.

Ditercalinium (Fig. 1), a 7*H*-pyridocarbazole dimer, is a synthetic anticancer drug that binds to DNA by bis-intercalation and induces repair of DNA in both prokaryotic and eukaryotic cells (2–4). The noncovalent complexes formed by ditercalinium with DNA are incorrectly recognized as covalent lesions by cellular repair systems. In *Escherichia coli*, the *uvrABC* system is known to efficiently repair a variety of covalent DNA adducts. However, the reversible nature of DNA–ditercalinium complexes enables the drug to dissociate from a *uvrABC*–DNA assembly and form another complex with the original target DNA. In an analogous fashion, mitochondrial DNA in ditercalinium-treated eukaryotic cells is degraded by DNA repair. Thus repair of DNA–ditercalinium complexes is a futile process that continues endlessly. Treated eukaryotic cells repair themselves to death (4). Ditercalinium exhibits a relatively new and unexpected mechanism of cell death with potential as a cancer treatment that is only now being explored.

As with other antitumor drugs that bind to DNA, minor chemical modifications of ditercalinium strongly influence biological activity. Strong antitumor activity is observed only when 7*H*-pyridocarbazoles are dimerized (5). Other important factors include the position and hybridization of the nitrogen substituted with the linker (5, 6) and the rigidity (5)

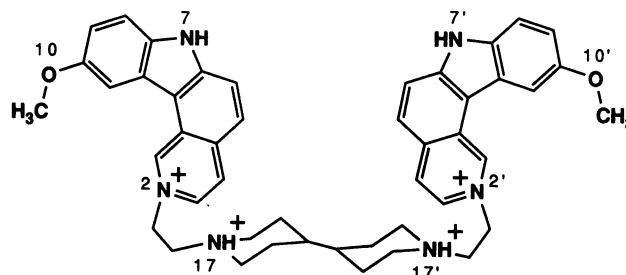


FIG. 1. Ditercalinium, with the labels on one half of the molecule marked with primes to indicate the lack of twofold symmetry in the complex with [d(CGCG)]₂.

and length (7) of the linker. Furthermore, the drug is inactivated when the N-7 position, or to a lesser extent the C-6 position, is substituted with alkyl groups larger than methyl (8), or when the position of the nitrogen at the 7 position within the chromophore is altered (5).

To understand the mechanisms of DNA repair induction by ditercalinium and why minor modifications of the drug result in dramatic changes in activity, we need to establish the details of how the drug interacts with and distorts DNA. Using x-ray crystallography, we have determined, to 1.7 Å resolution, the three-dimensional structure of a complex of ditercalinium bound to the double-stranded DNA fragment [d(CGCG)]₂.[§] A series of NMR studies of DNA–ditercalinium complexes by Roques and coworkers (9–13) has allowed us to compare those results with the x-ray structure described here. The three-dimensional structures of these DNA–drug complexes provide us with the potential to better understand the molecular basis of function and recognition in DNA repair processes.

MATERIALS AND METHODS

The self-complementary DNA tetramer d(CGCG) was synthesized by the phosphotriester method and purified with Sep-Pak C₁₈ cartridges (Waters). Ditercalinium was kindly supplied by Bernard P. Roques (Paris). Crystals were grown at room temperature in sitting drops by the vapor diffusion method. The crystallization mother liquor initially contained 0.7 mM DNA (single-strand concentration), 16.8 mM sodium cacodylate buffer (pH 6.0), 14 mM ammonium acetate, 0.3 mM spermine tetrahydrochloride, 0.8 mM magnesium chloride, 6% 2-methyl-2,4-pentanediol, and 0.2 mM ditercalinium. The sitting drops were equilibrated against a reservoir of 30% 2-methyl-2,4-pentanediol. Yellow tetragonal crystals

†Permanent address: Department of Structural Chemistry, Weizmann Institute of Science, Rehovot, Israel.

§The atomic coordinates and structure factors have been deposited in the Protein Data Bank, Chemistry Department, Brookhaven National Laboratory, Upton, NY 11973 (reference 1D32).

The publication costs of this article were defrayed in part by page charge payment. This article must therefore be hereby marked "advertisement" in accordance with 18 U.S.C. §1734 solely to indicate this fact.

began to appear in 1 week and within a month grew to a size of $0.28 \times 0.28 \times 0.35$ mm.

The space group and cell parameters were determined from precession photographs. The DNA–ditercalinium complex crystallized in space group $P4_12_12$ with unit cell dimensions $a = 26.88$ Å and $c = 82.60$ Å. X-ray diffraction data were collected at 0°C on a Rigaku AFC5 rotating anode diffractometer in the ω scan mode with $\text{CuK}\alpha$ radiation. Intensities were corrected for Lorentz, polarization, and absorption effects. A total of 2211 unique reflections with $F_{\text{obs}} > 3.0\sigma(F_{\text{obs}})$, with 542 reflections between 2.0 and 1.7 Å resolution, were included in the refinement. The strongest reflection (0 0 24) indicated that there were four DNA–ditercalinium complexes (with 24 planar groups, either base pairs or chromophores of ditercalinium) stacked 3.44 Å apart along the c axis. The complexes thus occupy general positions with the asymmetric unit consisting of one DNA duplex and one ditercalinium molecule.

Using the CpG intercalation step of the d(CGATCG)–Adriamycin (doxorubicin) complex (14) as a starting point, several models of the ditercalinium complex were constructed. Models were constructed with the ditercalinium linker in the major groove, or in the minor groove, or forming a network by connecting adjacent duplexes in the lattice. Using both ULTIMA (15) and the rotation/translation search routine of X-PLOR (16), models with the linker in the major groove resulted in the most favorable solutions. The two search programs gave the same solution, indicating the complex was located with its helical axis nearly coincident with the fourfold crystallographic screw axis.

The structure was refined with the Konnert–Hendrickson constrained least-squares refinement procedure (17) as modified for nucleic acids (18). Fourier electron density ($2F_{\text{obs}} - F_{\text{calc}}$) and difference electron density ($F_{\text{obs}} - F_{\text{calc}}$) maps were calculated and displayed on an Evans and Sutherland PS390 graphics terminal and manual manipulations of the models were performed with the program FRODO (19). During the refinement, the piperidine rings were constrained to the more stable chair conformations and the linker was rebuilt to fit into electron density maps. Each of the two possible rotamers of the two piperidine rings was placed into electron density maps. However, certain aspects of the conformation of one end of the linker remained ambiguous, and parallel refinements converged to the same R factors. It is possible that one

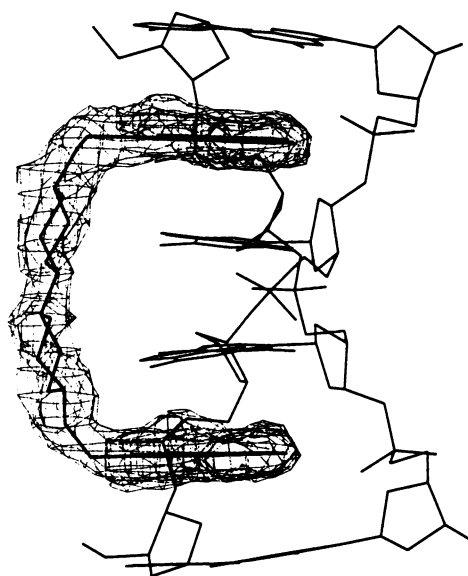


FIG. 2. Stick drawing of the $[\text{d}(\text{CGCG})]_2$ -ditercalinium complex showing the Fourier sum electron density ($2F_{\text{obs}} - F_{\text{calc}}$) surrounding the bis-intercalated drug.

end of the linker is disordered within the crystal. The ambiguity is localized in only one of the piperidine rings (on the end of ditercalinium that is not marked with primes in the figures). The thermodynamically most stable rotamer, shown in Fig. 2, was then selected. Water molecules were located from a series of difference electron density maps and were gradually added as the refinement progressed, resulting in a final R factor of 22.5%. The final asymmetric unit contains a complete $[\text{d}(\text{CGCG})]_2$ duplex, 1 ditercalinium molecule and 84 water molecules. The rms deviation from ideal bond lengths is 0.019 Å.

RESULTS

In the x-ray structure of ditercalinium bound to $[\text{d}(\text{CGCG})]_2$, the ditercalinium molecule bis-intercalates at the two CpG steps of the DNA fragment (see Figs. 2 and 4). The DNA retains an underwound, right-handed double-helical conformation with the linker of ditercalinium in the major groove as first shown by NMR (9–13). Although both the ditercalinium molecule and $[\text{d}(\text{CGCG})]_2$ have the potential to adopt twofold symmetry, the complex lacks symmetry in the x-ray structure. The conformation and DNA interactions of one half of the ditercalinium molecule are different from the other half.

The DNA in the complex with ditercalinium is kinked. This abrupt bend of $\approx 15^\circ$ in the helical axis toward the minor groove is clearly observable in Fig. 2. The kink appears to arise from a combination of several factors. First, torsional constraints of the linker prevent coplanarity of the two chromophores in the complex. Second, the large surface areas of the intercalated chromophores induce each base pair to be coplanar with the adjacent chromophore. Third, on the major groove side of the complex, the linker maintains an axial distance between the two chromophores (10.4 Å), which slightly exceeds the expected rise of 4 base pairs of B-DNA (10.2 Å). If the linker connecting the two bis-intercalated chromophores were flexible, we would expect the axial rise of the chromophores to be the same as the axial rise of 4 base pairs of B-DNA. The combined effects of the torsional constraints, the excess length of the rigid linker, and the large

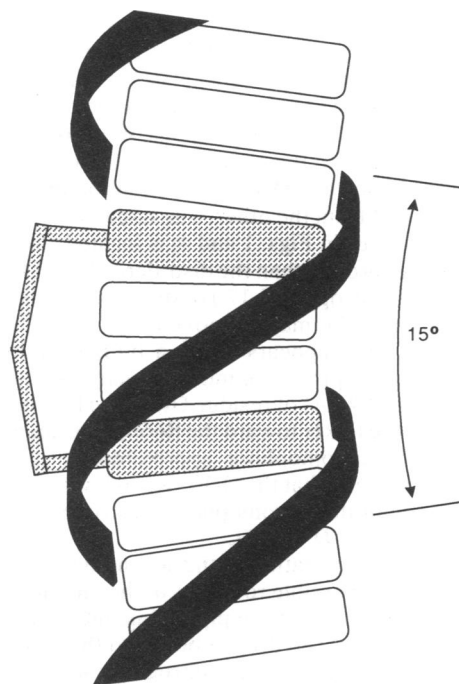


FIG. 3. Schematic diagram of a DNA–ditercalinium complex, illustrating the kink in the DNA helical axis induced by ditercalinium.

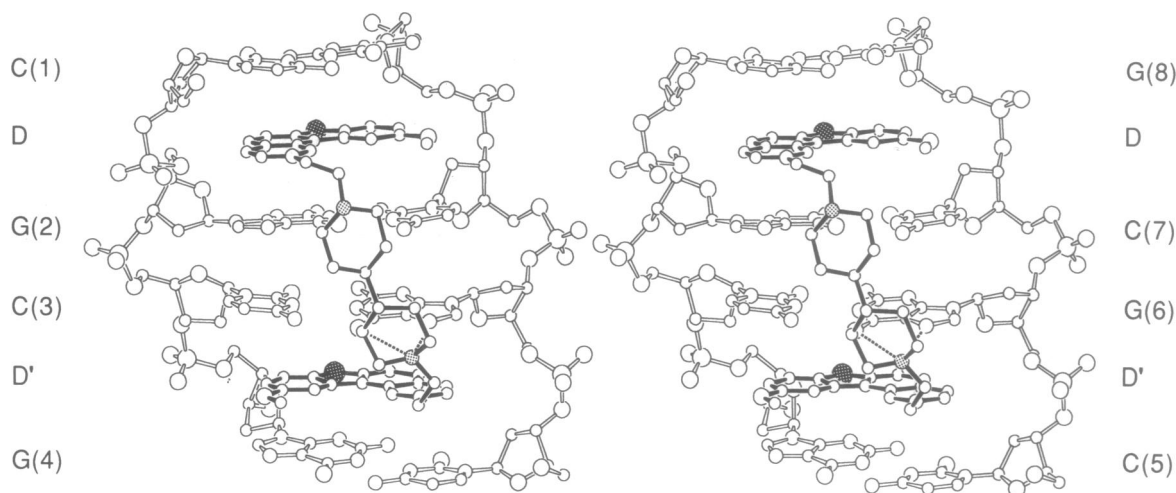


FIG. 4. ORTEP stereoview of the $[d(CGCG)]_2$ -ditercalinium complex viewed from the major groove. The DNA is drawn with open bonds and the ditercalinium is drawn with solid bonds. Hydrogen bonds between DNA and the N-17' atom of ditercalinium are drawn with dashed lines. Atom types are coded according to size with $P > O > N > C$ except the indole N-7 and N-7' atoms of ditercalinium, which are drawn as the largest circles and also marked with dark stippling. The piperidinic N-17 and N-17' atoms of ditercalinium are marked with light stippling.

surface areas of the intercalated chromophores are shown schematically in Fig. 3.

The DNA in the complex with ditercalinium is severely underwound. The helical twist is 22° at the first step, 30° at the second step, and 20° at the third step of the DNA tetramer. Compared to B-DNA, which averages a helical twist of 36° per step, the total extent of DNA unwinding is 36° in the fragment of DNA complexed with ditercalinium. The helical unwinding is observable in the axial views of successive base-pair-chromophore steps and base-pair-base-pair steps (see Fig. 5).

The kinking and unwinding of the DNA is accompanied by broadening of both grooves. For example, in the ditercalinium complex the P4 to P8 distance (minus 5.8 \AA , the van der Waals radii of the phosphate groups) is 10.5 \AA , while the width of the minor groove of B-DNA, as indicated by distances between analogous phosphates, is 5.7 \AA . Similarly, in the ditercalinium complex the P2 to P6 distance (minus the van der Waals radii of the phosphate groups) is 14.0 \AA , while the width of the major groove of B-DNA, as indicated by distances between analogous phosphates, is 11.7 \AA .

The linker of ditercalinium is located in the major groove. Although certain conformational details of one of the pyridyl rings remains unclear in the electron density maps, it is clear that the conformation and DNA interactions of one half of the linker are different from the other. The fixed half of the linker (marked with primes in Figs. 1 and 4) is located closer to the floor of the major groove than the disordered half. The proton of the piperidinic nitrogen (N-17') of the fixed ring is directed toward the floor of the major groove (Figs. 4 and 5D). This nitrogen forms what appears to be a bifurcated hydrogen bond, donating a proton simultaneously to both N-7 (2.95 \AA) and O-6 (3.44 \AA) of residue G(6). The hydrogen bond pulls the end of the linker toward the floor of the major groove and swivels the chromophore approximately around the DNA helical axis such that the O-10' methyl, which is located on the other end of this chromophore, protrudes out into the major groove (Fig. 5D and E).

Although the conformation of the second pyridyl ring may be disordered (two possible rotamers of the piperidine ring fit the density), it is clear that the piperidinic nitrogen (N-17) of this ring does not form hydrogen bonds to the DNA. At the current stage of refinement, this nitrogen is 4.81 \AA from the N-7 and 3.94 \AA from the O-6 of residue G(2). Furthermore, the proton on N-17 appears to be directed out, away from the floor of the major groove. In comparison with the hydrogen-

bonded end of the linker, the absence of a hydrogen bond from N-17 to the G(2)-C(7) base pair accompanies an increase in the distance between the linker and the base pair. This enables the O-10 methyl, unlike the O-10' methyl (described above), to stack on an adjacent cytosine base (Fig. 5B).

Ditercalinium bis-intercalates with the rigid linker in the major groove. The linker runs diagonally across the major groove such that the drug takes on the appearance of a backwards Z when viewed from the major groove (Figs. 4 and 6A). The linker runs counter to the twist of the DNA helix. The long axis of each of the chromophores is oriented nearly parallel to those of the flanking base pairs. The indole N-7-H and N-7'-H groups of the chromophores of ditercalinium are directed out toward the minor groove and are juxtaposed near the N-2 atoms of guanines when viewing down the helical axis (Fig. 5). The N-7 and N-7' atoms are flush with the floor of the minor groove and do not protrude into the groove. The view into the minor groove reveals the close mimicry of DNA base pairs by the drug molecule (Fig. 6B). The N-7 and N-7' atoms of ditercalinium appear to simulate N-2 atoms of guanines or N-3 atoms of adenines.

In the first step, viewing roughly along the helical axis (Fig. 5A), the cytosine base of C(1) is stacked directly on the pyridyl ring of the ditercalinium chromophore, while the guanosine base of G(8) is partially stacked on the indole and benzyl rings. In the second step, the guanine base of residue G(2) is nearly completely stacked on the pyridyl and benzyl rings, while the cytosine is only partially stacked on the O-10 methyl group (Fig. 5B). In the third step, the axial view (Fig. 5C) indicates good stacking of the C(3)-G(6) base pair with the G(2)-C(7) base pair. In the fourth step, the guanine base of G(6) is nearly completely stacked on the chromophore, while the complementary cytosine base of C(3) is less well stacked (Fig. 5D). The O-10' methyl of ditercalinium is unstacked and protrudes out into the major groove. In the fifth step (Fig. 5E), the cytosine base of C(5) is nearly completely stacked on the chromophore although not as well as C(1), the other terminal cytosine (Fig. 5A). The guanine base of G(4) is less well stacked than the complementary cytosine. In the van der Waals representation, the gaps between the ditercalinium chromophores and the terminal C-G base pairs (Fig. 6) indicate that the shapes of ditercalinium and the intercalation cavity within the DNA fragment are not closely matched.

DISCUSSION

Ditercalinium is a synthetic bis-intercalator with high affinity for DNA and strong antitumor properties. We describe the

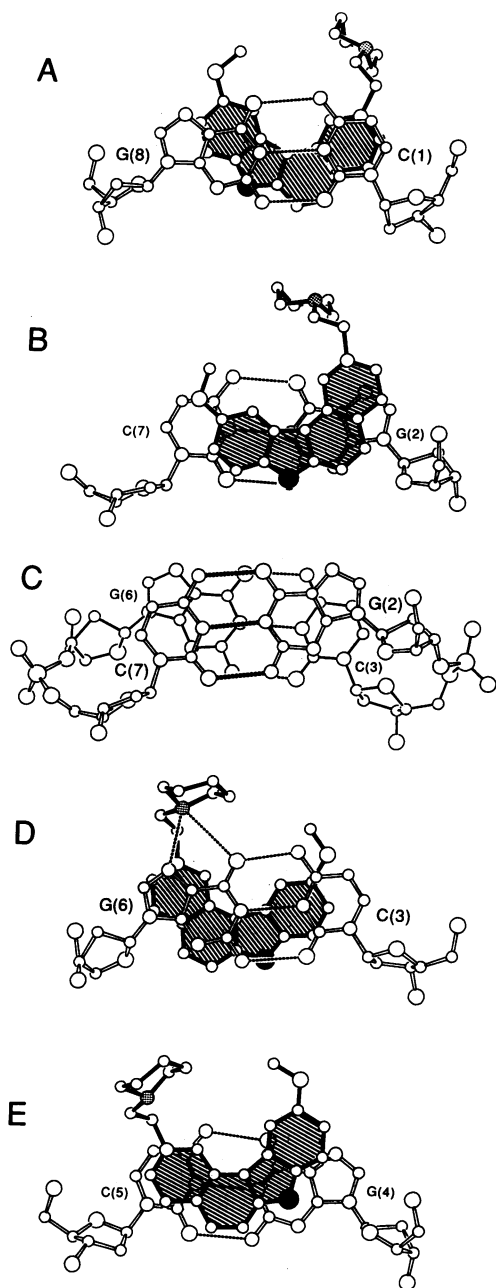


FIG. 5. Base-pair-chromophore steps and base-pair-base-pair steps of the $[d(CGCG)]_2$ -ditercalinium complex viewed along the normal of the best plane of either the upper base pair or the appropriate chromophore of ditercalinium. (A) The terminal C(1)-G(8) base pair on top of a chromophore of ditercalinium. (B) A chromophore of ditercalinium on top of the G(2)-C(7) base pair. (C) The G(2)-C(7) base pair on top of the C(3)-G(6) base pair. (D) The C(3)-G(6) base pair on top of a chromophore of ditercalinium. (E) A chromophore of ditercalinium on top of the G(4)-C(5) base pair. The major groove is directed toward the top of the figure and the minor groove is directed toward the bottom. The ditercalinium molecule is shaded and drawn with solid bonds, the closer DNA residues are drawn with open bonds, and the remote residues are drawn with thin bonds. The hydrogen bonds between the closer bases and from the N-17 atom of ditercalinium to the O-6 and N-7 atoms of G(6) are thick dashed lines; hydrogen bonds between remote bases are thin dashed lines. Atom types are coded according to size with $P > O > N > C$ except the indole N-7 and N-7' atoms of ditercalinium, which are drawn as the largest circles and marked with dark stippling. The piperidinic N-17 and N-17' atoms of ditercalinium are marked with light stippling. The labels of the residues that are closer to the viewer are larger than those of residues that are remote from the viewer.

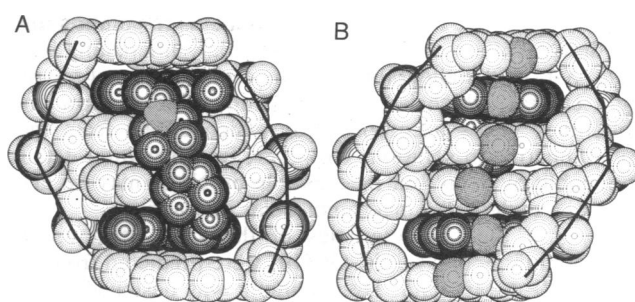


FIG. 6. Space filling representations of the major groove (A) and the minor groove (B) of the $[d(CGCG)]_2$ -ditercalinium complex. Each atom of the DNA is dotted except the phosphorus atoms, which are marked by concentric circles. The DNA sugar-phosphodiester backbones are traced with a solid black line and the ditercalinium molecule is darkened. The N-17 atom of ditercalinium is shaded; the N-17' atom, which forms hydrogen bonds to the major groove of the DNA, is obscured. (B) The N-7 and N-7' atoms of ditercalinium and the N-2 atoms of guanines are shaded to illustrate the DNA-like hydrogen bond donor pattern of the minor groove of the DNA-ditercalinium complex.

three-dimensional x-ray structure of a DNA-ditercalinium complex, which is a substrate of a DNA repair system. X-ray structures of ditercalinium and other substrates of DNA repair systems will be increasingly important for understanding mechanisms of repair. Ditercalinium activates DNA repair processes in both prokaryotic and eukaryotic cells. In prokaryotes, the DNA complex of ditercalinium is incorrectly recognized by the *uvrABC* repair system as a covalent lesion on DNA. A diverse array of covalent damage to DNA is excised by the *uvrABC* repair system (reviewed in ref. 1). *uvrABC* excises pyrimidine dimers, 6-4 photoadducts, and chemical adducts of psoralen, cisplatin, mitomycin C, benz[*a*]pyrene, and other reactive chemicals. In general, the damage excised by *uvrABC* causes distortions of DNA. The diversity of the covalent damage excised by *uvrABC* suggests that the DNA distortions are recognized by *uvrABC* rather than intrinsic structural motifs of the adducts. However, not all DNA distortions are recognized. *uvrABC* does not repair mispaired bases, *O*⁶-methylguanine, or 3-methyladenine. To account for *uvrABC* recognition of such a diverse array of DNA lesions, it has been proposed (1) that *uvrABC* recognizes DNA kinks and binds to the face of the DNA that does not contain the adduct.

The DNA in the complex with ditercalinium is kinked (by 15°) and severely unwound (by 36°) with exceptionally wide major and minor grooves. If *uvrABC* does recognize kinked DNA and bind to the undamaged face, the repair system would recognize the DNA kink induced by ditercalinium and bind to the minor groove of the complex where the shape and hydrogen bonding pattern mimics that of normal (undamaged) DNA. The two chromophores of a ditercalinium molecule substitute for two DNA base pairs with the N-7 and N-7' atoms of ditercalinium replacing N-2 atoms of guanines or N-3 atoms of adenines. The loss of activity of certain 7-substituted analogues of ditercalinium could then result from loss of *uvrABC* binding within the minor groove where the complexes would differ significantly from the minor groove of DNA, both in shape and in arrangement of hydrogen bonding functionalities.

A series of NMR studies of DNA-ditercalinium complexes (9-13) allow comparison of those results with the x-ray structure described here. A detailed comparison of a three-dimensional x-ray structure to an analogous NMR structure is impossible as the NMR data were not used to quantify interatomic distances. In general, NMR spectroscopy and x-ray crystallography are in many ways complementary techniques for the analysis of biological conformation. NMR

has the advantage of making measurements in solution and can detect kinetic events on a biologically interesting time scale. X-ray crystallography has the disadvantage of requiring a crystal, which is frequently impossible to grow and sometimes yields a conformation which differs from that predominating in solution. However, fine structural details obtainable by x-ray but inaccessible by NMR may be necessary to understand macromolecular interactions.

Many of the characteristics of the x-ray structure of ditercalinium bound to $[d(CGCG)]_2$ were predicted from the 1H and ^{31}P NMR data. Ditercalinium was designed with a rigid linker to prevent intramolecular interactions (self-stacking between chromophores) that would compete with DNA binding and decrease DNA affinity. The NMR experiments demonstrated that ditercalinium bis-intercalates in right-handed $[d(CGCG)]_2$ with the bases in the *anti* conformation and the linker of ditercalinium in the major groove. Additional important features such as the kink in the helical axis, the details of the stacking interactions, especially the differences between the two chromophores, and the hydrogen bonds between the linker and the major groove were observed crystallographically but were not apparent from the NMR experiments. It is interesting that a molecular mechanics study (20) of ditercalinium bound to $[d(CGCG)]_2$ did anticipate many aspects of the major groove hydrogen bonding scheme observed in the x-ray structure.

The positively charged nitrogens of ditercalinium are located near the floors of the major groove of the DNA. Favorable charge-charge interactions within the grooves of DNA appear to be an important factor in stability and conformation of complexes. The floors of the grooves are regions of DNA with the greatest electronegative potential (21). X-ray crystallographic studies suggest that mono- and polyamines uniformly bind to DNA so that the positive charges reside near the floors of the major or minor grooves. Positive charge is located near the floors of the grooves in the three-dimensional crystal structures of DNA complexed with (i) intercalators that place positive charge in the major (22, 23) or in the minor groove (14, 24, 25), (ii) minor groove binding compounds (26), and (iii) spermine in the major groove of A-DNA (27) and in the major groove of DNA-anthracycline complexes (24). Thus, placement of charged groups may be a primary consideration of designing agents that bind to DNA.

We would like to know which features of DNA-ditercalinium complexes activate DNA repair systems. The present structure leads to a number of suggestions but provides no firm answers. Could it be that the fixed 15° kink in the helical axis of the DNA-ditercalinium complex is similar to helical distortions resulting from covalent modifications? This is possible, but additional factors must be considered including other helical distortions and, in the minor groove, the unusual mimicry of base pairs by the chromophores of ditercalinium. We would hope to obtain answers to these questions by solving the crystal structures of DNA complexes of ditercalinium derivatives that do not induce DNA repair responses.

We thank Dr. Bernard P. Roques for the gift of the ditercalinium and Drs. Christin Frederick and Zippora Shakked for helpful discussions. This research was supported by grants from the National Institutes of Health, the American Cancer Society, the National

Science Foundation, the Office of Naval Research, and the National Aeronautics and Space Administration. L.D.W. acknowledges fellowship support by the National Institutes of Health. M.E. acknowledges fellowship support by the Geigy-Jubiläums-Stiftung.

1. Sancar, A. & Sancar, G. B. (1988) *Annu. Rev. Biochem.* **57**, 29-67.
2. Lambert, B., Roques, B. P. & Le Pecq, J. B. (1988) *Nucleic Acids Res.* **16**, 1063-1078.
3. Lambert, B., Jones, B. K., Roques, B. P., Le Pecq, J. B. & Yeung, A. T. (1989) *Proc. Natl. Acad. Sci. USA* **86**, 6557-6561.
4. Lambert, B., Segal-Bendirdjian, E., Esnault, C., Le Pecq, J. B., Roques, B. P., Jones, B. & Yeung, A. T. (1990) *Anti-Cancer Drug Des.* **5**, 43-53.
5. Pelaprat, D., Delbarre, A., Le Guen, I., Roques, B. P. & Le Pecq, J. B. (1980) *J. Med. Chem.* **23**, 1336-1343.
6. Léon, P., Garbay-Jaureguiberry, C., Barsi, M. C., Le Pecq, J. B. & Roques, B. P. (1987) *J. Med. Chem.* **30**, 2074-2080.
7. Garbay-Jaureguiberry, C., Laugaa, P., Delepierre, M., Laalam, S., Muzard, G., Le Pecq, J. B. & Roques, B. P. (1987) *Anti-Cancer Drug Des.* **1**, 323-335.
8. Léon, P., Garbay-Jaureguiberry, C., Le Pecq, J. B. & Roques, B. P. (1988) *Anti-Cancer Drug Des.* **3**, 1-13.
9. Delbarre, A., Delepierre, M., Igolen, J., Le Pecq, J. B. & Roques, B. P. (1985) *Biochimie* **67**, 823-828.
10. Delbarre, A., Delepierre, M., Langlois D'Estaintot, B., Igolen, J. & Roques, B. P. (1987) *Biopolymers* **26**, 1001-1033.
11. Delbarre, A., Delepierre, M., Garbay, C., Igolen, J., Le Pecq, J. B. & Roques, B. P. (1987) *Proc. Natl. Acad. Sci. USA* **84**, 2155-2159.
12. Delepierre, M., Igolen, J. & Roques, B. P. (1988) *Biopolymers* **27**, 957-968.
13. Delepierre, M., Maroun, R., Garbay-Jaureguiberry, C., Igolen, J. & Roques, B. P. (1989) *J. Mol. Biol.* **210**, 211-228.
14. Frederick, C. A., Williams, L. D., Ughetto, G., van der Marel, G. A., van Boom, J. H., Rich, A. & Wang, A. H.-J. (1990) *Biochemistry* **29**, 2538-2549.
15. Rabinovich, D. & Shakked, Z. (1984) *Acta Crystallogr. Sect. A* **40**, 195-200.
16. Brunger, A. (1988) *X-PLOR Software* (The Howard Hughes Medical Institute/Yale Univ., New Haven, CT).
17. Hendrickson, W. A. & Konnert, J. H. (1981) in *Biomolecular Structure, Conformation, Function, and Evolution*, ed. Srinivasan, R. (Pergamon, Oxford), Vol. 1, pp. 43-57.
18. Quigley, G. J., Teeter, M. M. & Rich, A. (1978) *Proc. Natl. Acad. Sci. USA* **75**, 64-68.
19. Jones, T. A. (1982) in *Computational Crystallography*, ed. Sayre, D. (Clarendon, Oxford), Vol. 11, pp. 303-317.
20. Maroun, R., Delepierre, M. & Roques, B. P. (1989) *J. Biomol. Struct. Dyn.* **7**, 607-621.
21. Lavery, R. & Pullman, B. (1985) *J. Biomol. Struct. Dyn.* **2**, 1021-1032.
22. Williams, L. D., Egli, M., Gao, Q., Bash, P., van der Marel, G. A., van Boom, J. H., Rich, A. & Frederick, C. A. (1990) *Proc. Natl. Acad. Sci. USA* **87**, 2225-2229.
23. Egli, M., Williams, L. D., Frederick, C. A. & Rich, A. (1991) *Biochemistry*, in press.
24. Williams, L. D., Frederick, C. A., Ughetto, G. & Rich, A. (1990) *Nucleic Acids Res.* **18**, 5533-5541.
25. Williams, L. D., Egli, M., Ughetto, G., van der Marel, G. A., van Boom, J. H., Quigley, G. J., Wang, A. H.-J., Rich, A. & Frederick, C. A. (1990) *J. Mol. Biol.* **215**, 313-320.
26. Coll, M., Frederick, C. A., Wang, A. H.-J. & Rich, A. (1987) *Proc. Natl. Acad. Sci. USA* **84**, 8385-8389.
27. Jain, S., Zon, G. & Sundaralingam, M. (1989) *Biochemistry* **28**, 2360-2364.